BASIC AND TRANSLATIONAL SCIENCES

Circadian Rhythmicity in Cerebral Microvascular Tone Influences Subarachnoid Hemorrhage–Induced Injury

Darcy Lidington ©, PhD*; Hoyee Wan, PhD*; Danny D. Dinh, PhD; Chloe Ng ©, MSc; Steffen-Sebastian Bolz ©, MD, PhD

BACKGROUND AND PURPOSE: Circadian rhythms influence the extent of brain injury following subarachnoid hemorrhage (SAH), but the mechanism is unknown. We hypothesized that cerebrovascular myogenic reactivity is rhythmic and explains the circadian variation in SAH-induced injury.

METHODS: SAH was modeled in mice with prechiasmatic blood injection. Inducible, smooth muscle cell–specific Bmal1 (brain and muscle aryl hydrocarbon receptor nuclear translocator-like protein 1) gene deletion (smooth muscle–specific Bmal1 1 knockout [sm-Bmal1 KO]) disrupted circadian rhythms within the cerebral microcirculation. Olfactory cerebral resistance arteries were functionally assessed by pressure myography in vitro; these functional assessments were related to polymerase chain reaction/Western blot data, brain histology (Fluoro-Jade/activated caspase-3), and neurobehavioral assessments (modified Garcia scores).

RESULTS: Cerebrovascular myogenic vasoconstriction is rhythmic, with a peak and trough at Zeitgeber times 23 and 11 (ZT23 and ZT11), respectively. Histological and neurobehavioral assessments demonstrate that higher injury levels occur when SAH is induced at ZT23, compared with ZT11. In sm-Bmal1 KO mice, myogenic reactivity is not rhythmic. Interestingly, myogenic tone is higher at ZT11 versus ZT23 in sm-Bmal1 KO mice; accordingly, SAH-induced injury in sm-Bmal1 KO mice is more severe when SAH is induced at ZT11 compared to ZT23. We examined several myogenic signaling components and found that CFTR (cystic fibrosis transmembrane conductance regulator) expression is rhythmic in cerebral arteries. Pharmacologically stabilizing CFTR expression in vivo (3 mg/kg lumacaftor for 2 days) eliminates the rhythmicity in myogenic reactivity and abolishes the circadian variation in SAH-induced neurological injury.

CONCLUSIONS: Cerebrovascular myogenic reactivity is rhythmic. The level of myogenic tone at the time of SAH ictus is a key factor influencing the extent of injury. Circadian oscillations in cerebrovascular CFTR expression appear to underlie the cerebrovascular myogenic reactivity rhythm.

GRAPHIC ABSTRACT: A graphic abstract is available for this article.

Key Words: brain injury ■ circadian rhythm ■ cystic fibrosis transmembrane conductance regulator ■ lumacaftor ■ subarachnoid hemorrhage

A neurysmal subarachnoid hemorrhage (SAH) is a devastating stroke subtype that kills over half of those afflicted and permanently debilitates half of the surviving patients.[1] In experimental settings, the time of day that SAH occurs significantly impacts the extent of neuronal injury that subsequently ensues.[2] This is not surprising, since: (1) numerous cellular processes are under circadian control[3,4] and (2) circadian clock disruption is known to worsen outcomes in other brain injury models, including traumatic brain injury.[5] Nevertheless,

Stroke is available at www.ahajournals.org/journal/str

Nonstandard Abbreviations and Acronyms

Bmal1	brain and muscle aryl hydrocarbon receptor nuclear translocator-like protein 1
CFTR	cystic fibrosis transmembrane conductance regulator
Iba-1	ionized calcium-binding adaptor molecule 1
S1P	sphingosine-1-phosphate
S1P2R	sphingosine-1-phosphate receptor 2
SAH	subarachnoid hemorrhage
sm-Bmal1 KO	smooth muscle–specific Bmal1 knockout
Sphk1	sphingosine kinase 1
WT/Cre	Cre-expressing wild-type control (tamoxifen treated)
ZT11	Zeitgeber time 11
ZT23	Zeitgeber time 23

the specific underlying mechanism driving this circadian difference in SAH-induced injury remains elusive.

Our recent work demonstrates that the cerebral microcirculation plays a central role in SAH-induced injury.[6,7] Small (<300 µm) resistance arteries that link the systemic circulation to the cerebral capillary beds are the chief regulators of cerebral perfusion[8] and thus, represent a key therapeutic target for clinically mitigating SAH injury. Cerebral resistance artery myogenic reactivity, the primary mechanism underlying cerebral blood flow autoregulation, is profoundly augmented following SAH: this results in perfusion deficits that strongly associate with neurological injury.[6,7] Interestingly, several studies demonstrate that cerebral perfusion is under circadian control, with higher perfusion levels occurring during wakeful periods.[9,10] Although this could represent differences in metabolic demand and neurovascular coupling during wakefulness,[11] it is equally conceivable that circadian oscillations in cerebrovascular reactivity drive the cerebral perfusion rhythm. Circadian oscillations in cerebrovascular reactivity may also explain why many cerebrovascular events (eg, stroke, transient ischemic attack) also display a circadian pattern in their time of onset.[12]

Given the strong association we established between cerebral resistance artery myogenic reactivity, cerebral perfusion, and neuronal injury in SAH,[6,7] we hypothesized that circadian variations in cerebrovascular constriction underpin the time-of-day variations in SAH-induced injury.[2] To address this hypothesis, we utilized a smooth muscle cell–specific circadian clock disruption model to (i) demonstrate the existence of a circadian rhythm in cerebrovascular myogenic reactivity and (ii) confirm that these oscillations in cerebrovascular tone influence the extent of SAH-induced brain injury.

METHODS

The data supporting the findings of this study are available from the corresponding author upon reasonable request. This investigation conforms to the National Research Council's 2011 Guide for the Care and Use of Laboratory Animals (International Standard Book Number [ISBN]: 0-309-15400-6). All experimental procedures were approved by the Institutional Animal Care and Use Committee at the University of Toronto.

Mice

Wild-type mice (C57BL/6N) were purchased from Charles River Laboratories (Montreal, Canada). Inducible, smooth muscle cell-targeted Bmal1 (brain and muscle aryl hydrocarbon receptor nuclear translocator-like protein 1) knockout mice (sm-Bmal1 KO) were generated by crossing floxed Bmal1 mice[13] with mice expressing a recombinant Cre recombinase under the control of a smooth muscle promoter (SMMHC-CreER[T2])[14]; both founder strains are commercially available at Jackson Laboratories (Bar Harbor). Deletion of the floxed *Bmal1* gene was achieved with 3 days of tamoxifen treatment (1 mg/day IP dissolved in corn oil; Millipore Sigma Canada, Oakville Canada, catalog no. T5648 and C8267). Tamoxifen-treated littermates expressing CreER[T2] and nonfloxed *Bmal1* alleles served as wild-type controls (Cre-expressing wild-type control [tamoxifen treated; WT/Cre]). All mice were housed in a controlled climate (21 °C, 40%–60% humidity) with a standard 12-hour:12-hour light-dark cycle, fed normal chow, and had ad libitum access to water and food. The mice were used for experiments at 8-12 weeks of age. Animal euthanization was completed using 5% isoflurane.

Induction of Subarachnoid Hemorrhage

We utilized a well-characterized blood injection model of SAH.[6] Surgeries were completed within 30 minutes of Zeitgeber time 11 (ZT11) and Zeitgeber time 23 (ZT23); surgeries at ZT23 were conducted under red light illumination to eliminate the impact of light on the entrained circadian rhythm. Briefly, all mice received a single preoperative dose of sustained-release buprenorphine (1.0 mg/kg SC). Each mouse was anesthetized (5% isoflurane induction, 1%–2% maintenance) and fixed in a stereotactic frame. A 7 mm incision was made along the midline of the anterior scalp and a 0.9 mm hole was drilled into the skull 4.5 mm anterior to the bregma. A spinal needle was advanced to the prechiasmatic cistern and 80 µL of arterial blood from a syngeneic donor mouse, obtained by cardiac puncture, was injected into the intracranial space over 10 seconds. Following injection, the scalp incision was closed and the mice recovered in heated cages. Experimental end points were collected at 48 hours post-SAH induction, as our previous studies demonstrate that both reduced cerebral perfusion and maximal changes in vascular reactivity occur at this time point.[6,7] Mortality associated with the SAH procedure was ≈2.5% (2 out of 75); 1 mouse in the WT/Cre ZT11 group sustained an injury from improper fixation in the stereotaxic frame and was excluded from analysis.

Pressure Myography

We utilized a well-characterized pressure myography approach, as previously described.[6,7] Briefly, mouse olfactory cerebral arteries were carefully dissected, cannulated

onto micropipettes, stretched to their in vivo lengths, pressurized, and warmed to 37 °C. Artery viability was assessed with 10 μmol/L phenylephrine: arteries failing to show ≥30% constriction were excluded. Myogenic and phenylephrine-stimulated tone were calculated as the percent constriction in relation to the maximal artery diameter. Additional details are provided in the Supplemental Material.

Histology

Brains were cleared of blood and fixed via aortic perfusion with 10% buffered formalin. Standard procedures were utilized to prepare slides with 5 μm thick paraffin coronal slices, starting at −2 mm from bregma.[6,7] Following staining, activated caspase-3/NeuN (neuronal nuclear protein) and Fluoro-Jade–positive cells were counted in the cortical region that included the left and right temporal and parietal lobes at ×20 magnification (1 slice assessed per mouse). For microglial activation assessments, we evaluated the expression of Iba-1 (ionized calcium-binding adaptor protein-1) in cortical and hippocampal tissue. The percentage of pixels above a preset threshold was reported as the positive area fraction for Iba-1 staining[15]; for cortical samples, microglial soma size was also measured.[16] Anterior cerebral artery constriction was quantified in hematoxylin/eosin–stained slides as the lumen radius / wall thickness ratio.[2] Not all slide preparations contained the anterior cerebral arteries, in which case, the slides were excluded from analysis. The procedures are described in detail in the Supplemental Material.

Neurological Function in SAH Mice

Neurological function was assessed utilizing the modified Garcia score, as previously described.[6,7] The neurological assessment consists of 6 domains: spontaneous activity, spontaneous movement of all 4 limbs, forepaw outstretching, climbing, body proprioception, and response to vibrissae touch. The maximum score is 18, indicative of normal neurological function. Modified Garcia assessments at ZT23 were conducted under red light conditions.

Western Blots and Quantitative Polymerase Chain Reaction

Standard procedures were utilized for CFTR (cystic fibrosis transmembrane conductance regulator) Western blots and quantitative real-time polymerase chain reaction.[7] Specific details are provided in the Supplemental Material; uncropped blots for all Western blot experiments are presented in Figures S1 and S2 in the Supplemental Material; polymerase chain reaction primers are described in Table S1 in the Supplemental Material.

Lumacaftor Treatment

Consistent with our previous work,[7] wild-type mice were treated with Lumacaftor (each intraperitoneal injection delivered 1.5 mg/kg in 50 μL dimethyl sulfoxide-containing vehicle; catalog no. 22196; Cayman Chemical, Michigan) or vehicle twice daily for 2 days before cerebral artery harvest or SAH surgery. The injections were administered at ZT8/ZT21 for the ZT11 group and ZT4/ZT17 for the ZT23 group. Lumacaftor was not administered on the SAH surgical day or thereafter.

Data Collection and Statistics

This study utilized 353 experimental mice and 76 blood donor mice. A complete cohort breakdown and experimental timeline appears in Tables S2 and S3 in the Supplemental Material. Only male mice were used in this study to ensure appropriate comparability, as the Cre transgene is located on the Y-chromosome.[14] Mice were randomly assigned into groups before interventions, without the use of an explicit randomization procedure. Using previous data as guidance, we calculated the experimental group sizes necessary to ensure that all data sets provide an 80% power level for the detection of the anticipated differences between groups with a two-tailed alpha level of 0.05.

Datasets were analyzed for normality (Shapiro-Wilk test) and variance homogeneity (F or Brown-Forsythe test) before statistical comparison. Data sets subjected to parametric statistical tests are presented as means±SD. Data sets subjected to nonparametric statistical analyses, including circadian rhythm analyses, are presented as median±interquartile range and are identified in the figure legend. In all cases, n represents the number of independent measures. Myogenic reactivity and phenylephrine curves were compared using a repeated two-way ANOVA with Greenhouse-Geisser correction (Graphpad Prism 9 software; San Diego). Circadian rhythms were identified using JTK_CYCLE (version 3.1) with R software (version 3.4.0), a nonparametric test designed to reliably identify rhythmicity.[17] All other data were analyzed with standard parametric (ie, unpaired Student t test and ANOVA) and nonparametric (Mann-Whitney, Kruskal-Wallis test) statistical tests with appropriate corrections, as required (Prism 9). All figure data and statistical test outcomes are numerically presented in Tables S4–S6 in the Supplemental Material; all JTK_CYCLE analyses are found in Table S7 in the Supplemental Material; in all cases, differences were considered significant at $P<0.05$.

Histological assessments were conducted under blinded conditions; all other end points were collected without blinding, as the assessment ZT times could not be concealed. There were no a priori exclusions for primary end points, except as stated above in pressure myography and histology subsections.

RESULTS

Oscillations in Cerebral Artery Myogenic Tone Influence SAH-Induced Injury

Cerebral artery myogenic vasoconstriction possesses a statistically significant circadian rhythm at all transmural pressures assessed, with a peak and trough at ZT23 and ZT11, respectively (Figure 1A). In contrast, phenylephrine-stimulated vasoconstriction is not rhythmic (Figure 1B), indicating that the circadian oscillator manipulates a myogenic response element, rather than altering general contractility. Smooth muscle cell–specific Bmal1 gene deletion eliminates the rhythm in myogenic reactivity (Figure 1C); phenylephrine-stimulated vasoconstriction remains arrhythmic (Figure 1D). This indicates that the smooth muscle cell peripheral molecular clock drives the myogenic reactivity rhythm. Intriguingly, although sm-Bmal1 KO cerebral arteries no longer possess a circadian rhythm in myogenic reactivity, the
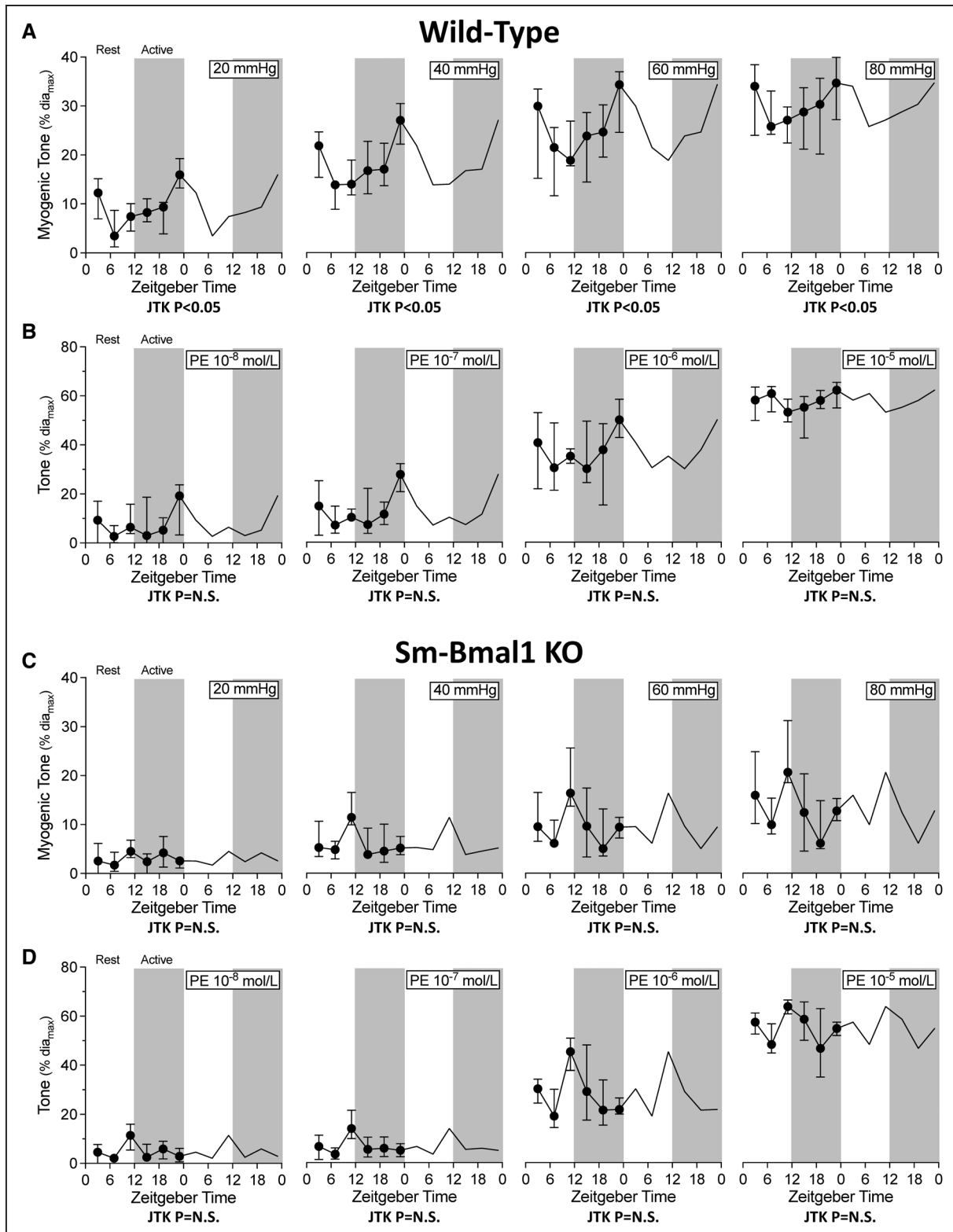
Figure 1. Cerebral artery myogenic responsiveness displays circadian rhythmicity.
Wild-type olfactory cerebral artery (**A**) myogenic tone and (**B**) phenylephrine (PE)-stimulated vasoconstriction are plotted over Zeitgeber time (n=6–8 at each Zeitgeber time point). **C**, Myogenic tone and (**D**) phenylephrine-stimulated vasoconstriction in olfactory cerebral arteries isolated from smooth muscle cell–specific Bmal1 (brain and muscle aryl hydrocarbon receptor nuclear translocator-like protein 1) knockout mice are plotted over Zeitgeber time (n=5–11 at each Zeitgeber time point). In wild-type arteries, myogenic tone at every transmural pressure exhibits a statistically significant circadian rhythm; smooth muscle cell–specific Bmal1 gene deletion (smooth muscle–specific Bmal1 1 knockout [sm-Bmal1 KO]) abolishes this rhythm. Data are presented as medians±interquartile range and are double-plotted for visualization purposes; white shading indicates lights on and dark shading indicates lights off. N.S. indicates not significant.

new profile displays an isolated peak in myogenic tone at ZT11 (Figure 1C), yielding an apparent inversion of the myogenic tone relationship between ZT11 and ZT23.

Higher cerebral artery myogenic tone would be expected to reduce brain perfusion: we, therefore, hypothesized that SAH-induced injury in WT/Cre mice should be higher at ZT23 compared to ZT11. Indeed, we observe a tight association between myogenic tone and SAH-induced brain injury (Figure 2). At 2 days post-SAH, Fluoro-Jade and activated caspase-3 positive cell counts are greater when SAH is induced at ZT23 versus ZT11; modified Garcia scores indicate significantly higher impairment in the ZT23 group. Strikingly, these parameters remain tightly aligned in the sm-Bmal1 KO model: myogenic vasoconstriction is higher at ZT11 versus ZT23 (Figure 3), as are Fluoro-Jade and activated caspase-3–positive cell counts following SAH; modified Garcia scores indicate greater impairment when SAH is induced at ZT11 versus ZT23 in sm-Bmal1 KO mice. Collectively, these results demonstrate a tight association between vascular reactivity at the time of SAH ictus and the injury level that subsequently ensues.

Microglial Activation and Large Artery Constriction Do Not Explain the Time-of-Day Difference in SAH-Induced Injury

Cortical Iba-1 expression was higher at ZT23 relative to ZT11 in WT/Cre mice, indicating increased microglial activation (Figure 4). Furthermore, consistent with previous observations by Schallner et al,[2] microglial cells displayed a more activated morphology at ZT23 compared to ZT11, as evidenced by larger soma size[16] (Figure S3 in the Supplemental Material). Remarkably, neither positive area fraction nor the soma size patterns change in the sm-Bmal1 KO setting (Figure 4 and Figure S3 in the Supplemental Material). A similar wild-type pattern is observed in the hippocampal region; however, the ZT11/ZT23 difference is lost in the sm-Bmal1 KO setting (Figure S4 in the Supplemental Material). Collectively, these data indicate that circadian differences in microglial activation do not explain the time-of-day injury difference in SAH. No difference in anterior cerebral artery vasoconstriction was detected in WT/Cre mice following SAH (Figure 4), indicating that microvascular
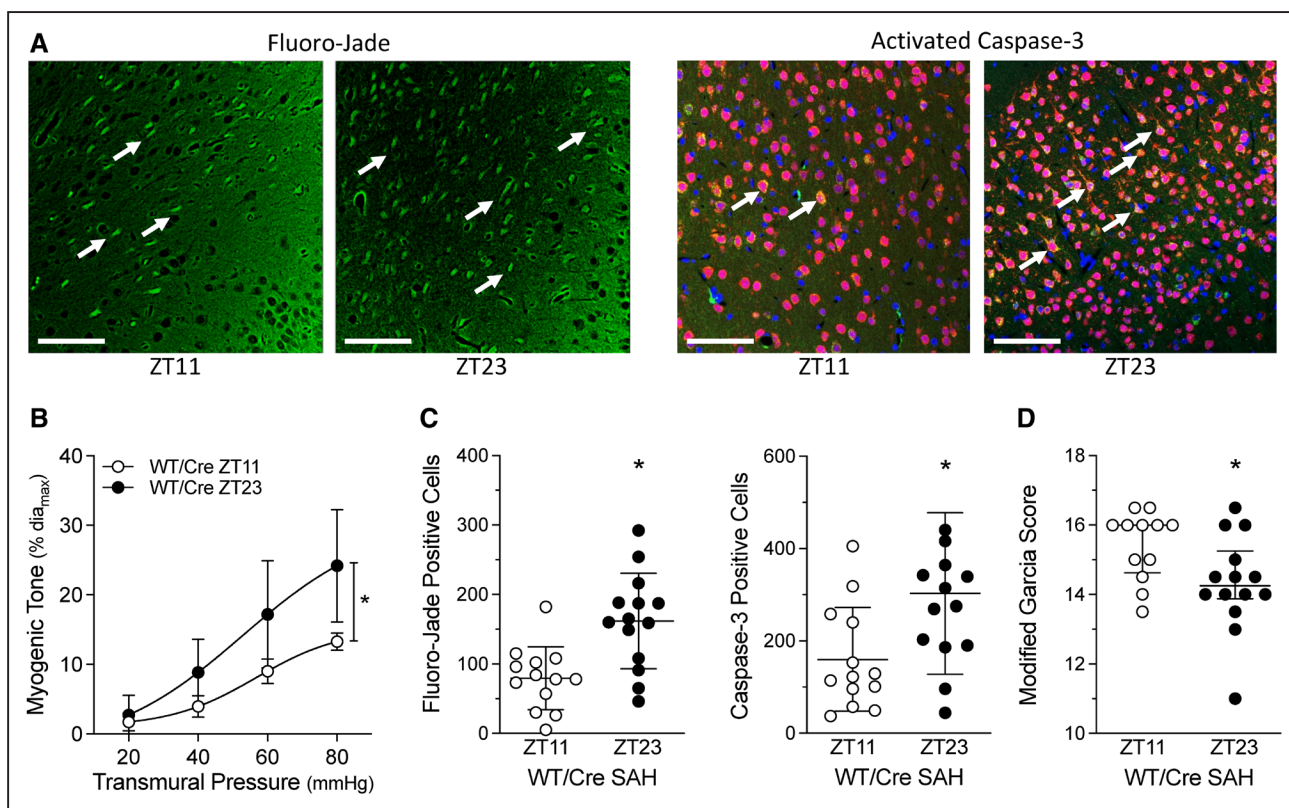

Figure 2. Subarachnoid hemorrhage (SAH)–induced injury associates with cerebral artery myogenic tone.
SAH was induced in tamoxifen-treated, Cre-expressing control mice (Cre-expressing wild-type control [tamoxifen treated; WT/Cre]) at Zeitgeber time 11 (ZT11) or Zeitgeber time 23 (ZT23); behavioral assessments and tissue collection were conducted 48 h afterwards. **A**, Representative images of cortical cells stained with Fluoro-Jade (**left**) and for activated caspase-3 expression (**right**); arrows point to positively stained cells (Bar=60 µm). **B**–**D**, Show the association between myogenic tone at the time of SAH and the resulting injury that ensues. **B**, Before the SAH surgery, olfactory cerebral artery myogenic tone is higher at ZT23, relative to ZT11 (n=5). **C**, Positive cell counts for Fluoro-Jade staining and activated caspase-3 are higher when SAH is induced at ZT23, relative to ZT11 (n=13–14). **D**, Modified Garcia scores are lower when SAH is induced at ZT23, relative to ZT11. Modified Garcia scores in **D** are presented as medians±interquartile range and compared with a Mann-Whitney test. *P<0.05.
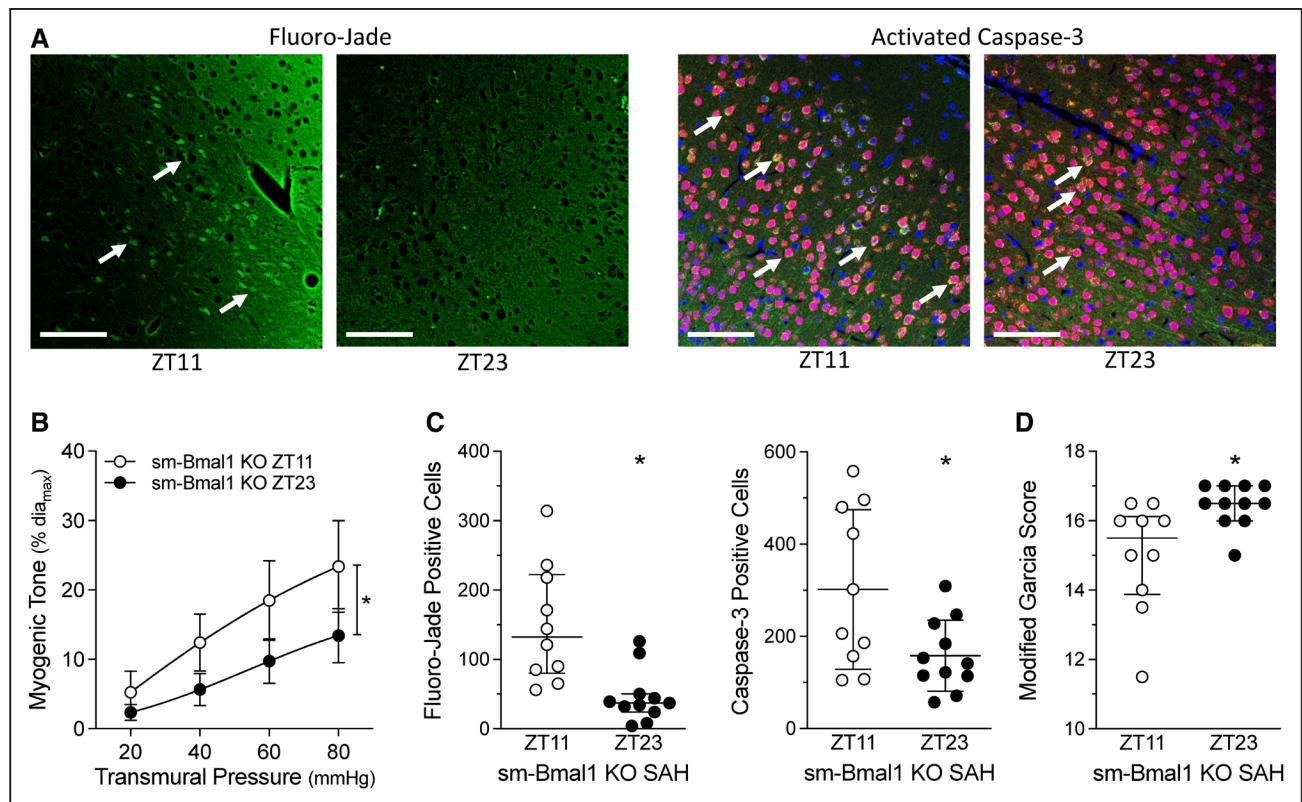
Figure 3. Subarachnoid hemorrhage (SAH)–induced injury in smooth muscle–specific Bmal1 (brain and muscle aryl hydrocarbon receptor nuclear translocator-like protein 1) knockout (sm-Bmal1 KO) mice.
SAH was induced in sm-Bmal1 KO at Zeitgeber time 11 (ZT11) or Zeitgeber time 23 (ZT23); behavioral assessments and tissue collection were conducted 48 h afterwards. **A**, Shows representative images of cortical cells stained with Fluoro-Jade (**left**) and for activated caspase-3 expression (**right**); arrows point to positively stained cells (Bar=60 µm). **B–D**, Show the association between myogenic tone at the time of SAH and the resulting injury that ensues. **B**, Before the SAH surgery, myogenic tone in sm-Bmal1 KO olfactory cerebral arteries is higher at ZT11, relative to ZT23 (n=6). **C**, Positive cell counts for Fluoro-Jade staining and activated caspase-3 are higher when SAH is induced at ZT11, relative to ZT23 in sm-Bmal1 KO mice (n=10–11). **D**, Modified Garcia scores in sm-Bmal1 KO mice are lower when SAH is induced at ZT11, relative to ZT23. Fluoro-Jade counts (**C**, **left**) and modified Garcia scores (**D**) are presented as medians±interquartile range and compared with a Mann-Whitney test; caspase-3 counts (**C**, **right**) were compared with a Welch-corrected t test. *$P<0.05$.

reactivity, rather than large artery vasoconstriction, is the primary determinant driving the time-of-day difference in SAH-induced injury.

Cerebral Artery CFTR Expression Is Oscillatory

We have previously demonstrated that the S1P (sphingosine-1-phosphate) signaling components Sphk1 (sphingosine kinase 1),[6] S1P$_2$R (S1P receptor 2),[6] and CFTR[7] all contribute to the regulation of cerebral artery myogenic reactivity. We, therefore, assessed whether any of these targets oscillate with a pattern that could explain the myogenic reactivity rhythm. The cerebral artery mRNA expression patterns for Bmal1, Per2 (period circadian regulator 2), and Clock (circadian locomotor output cycles kaput) (all core components of the molecular clock) are circadian (Figure S5 in the Supplemental Material), with peaks and troughs occurring at time points similar to those reported for aortic tissue.[18] Neither Sphk1 nor S1P$_2$R mRNA expression is rhythmic in cerebral arteries (Figure S5 in the Supplemental

Material); however, cerebral artery CFTR mRNA expression is rhythmic (Figure 5A) and persists when mice are housed under constant dark conditions (Figure S6 in the Supplemental Material). The peak and trough of CFTR mRNA expression is antiphase to the myogenic rhythm, consistent with CFTR's role as a negative regulator of myogenic reactivity.[7,19] At the protein level, CFTR is more highly expressed at ZT11 relative to ZT23 in WT/Cre arteries; this difference in expression is lost in sm-Bmal1 KO cerebral arteries (Figure 5B), indicating that the peripheral smooth muscle cell molecular clock drives the rhythm in CFTR expression, rather than external influences. As a technical limitation, we did not obtain knockout samples to confirm CFTR antibody specificity. The CFTR antibody used in the present study (1) reliably reproduced previous observations generated using CFTR antibodies from other manufacturers[6,7] and (2) yielded bands that aligned with a positive control from a heterologous expression system. Although we are confident that CFTR is being measured, the lack of knockout validation must be considered in the interpretation.
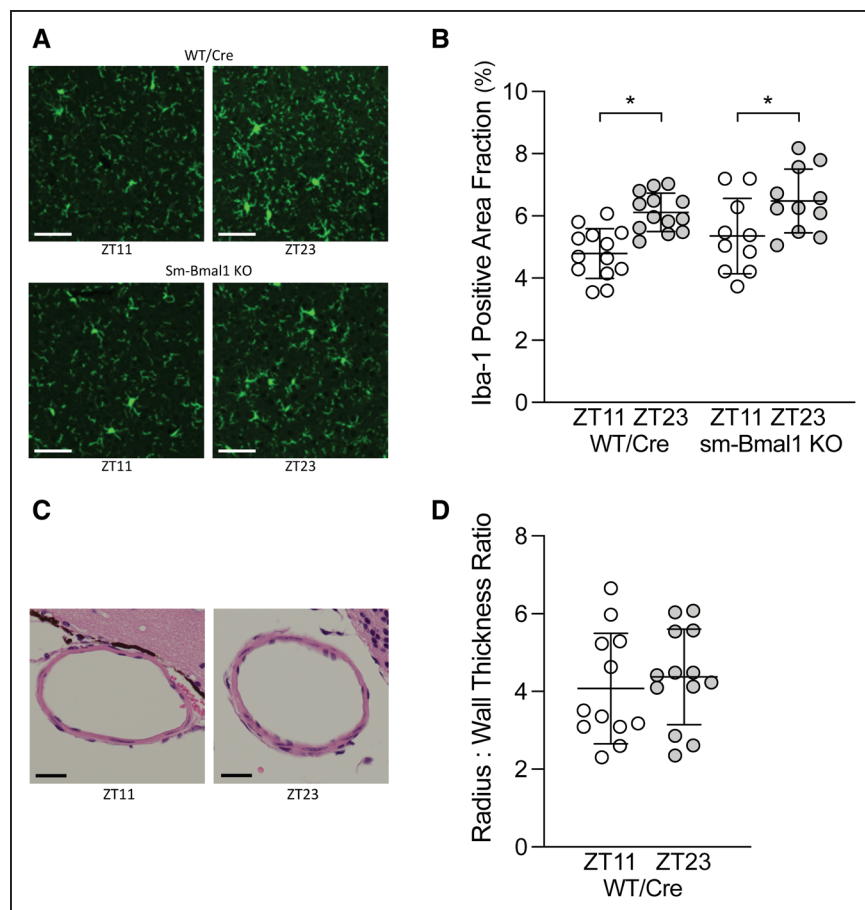
Figure 4. Influence of subarachnoid hemorrhage (SAH) onset time on microglial activation and anterior cerebral artery vasoconstriction. SAH was induced in tamoxifen-treated, Cre-expressing control (Cre-expressing wild-type control [tamoxifen treated; WT/Cre]) and smooth muscle cell–specific Bmal1 (brain and muscle aryl hydrocarbon receptor nuclear translocator-like protein 1) knockout (sm-Bmal1 KO) mice at Zeitgeber time 11 (ZT11) or Zeitgeber time 23 (ZT23); tissue collection was conducted 48 h afterward. **A**, Representative images of cortical cells stained with the microglial marker Iba-1 (ionized calcium-binding adaptor protein-1). Bar=60 μm. **B**, The images were quantified as the percentage area positive for Iba-1 staining relative to the field of view (ie, area fraction). In WT/Cre mice, Iba-1 staining occupies a larger fraction (ie, higher microglial cell activation) when SAH is induced at ZT23, relative to ZT11 (n=13); this relationship does not change in sm-Bmal1 KO mice (n=10–11). **C**, Representative cross-sections of the anterior cerebral artery (Bar=20 μm) and (**D**) accompanying vasoconstriction assessment, defined as the lumen radius: wall thickness ratio. No difference in large artery vasoconstriction is observed. *P<0.05 for the respective ZT11/ZT23 comparison.

The CFTR protein expression rhythm drives a functionally relevant change in CFTR activity, as exhibited by the time-dependent effect of specific CFTR inhibition (100 nmol/L $CFTR_{(inh)}$-172). CFTR inhibition attenuates myogenic tone at ZT11 (Figure 5C; ie, when CFTR expression is high) but not at ZT23 (Figure 5D; ie, when CFTR expression is low). The reduction in myogenic tone following $CFTR_{(inh)}$-172 treatment is most reasonably explained as a blockade of an outward chloride current (Figure S7 in the Supplemental Material), as previously described.[20]

Lumacaftor Abolishes the Circadian Rhythm in Cerebral Artery Myogenic Vasoconstriction and Eliminates the Time-of-Day Difference in SAH-Induced Injury

Lumacaftor treatment (3 mg/kg for 2 days) in naïve wild-type mice increases cerebral artery CFTR protein expression at ZT23; intriguingly, CFTR expression at ZT11 does not increase relative to the vehicle-treated control (Figure 5E). Lumacaftor treatment abolishes the rhythm in cerebral artery myogenic reactivity (Figure 5F), consistent with the lack ZT11/ZT23 CFTR protein expression difference. The level of cerebral artery myogenic tone observed in Figure 5F approximates the ZT11 level in Figure 2B. Lumacaftor treatment does

not appreciably affect phenylephrine-stimulated vasoconstriction, which remains arrhythmic (Figure S8 in the Supplemental Material). Consistent with the tight association between myogenic tone and injury following SAH, lumacaftor pretreatment abolishes the time-of-day differences in Fluoro-Jade and activated caspase-3 positive cells and modified Garcia scores at 2 days post-SAH (Figure 6).

DISCUSSION

Using a smooth muscle cell–specific circadian clock disruption model, we provide compelling evidence that cerebrovascular myogenic reactivity is rhythmic and drives time-of-day differences in SAH injury. Our data further suggest that this cerebrovascular rhythm arises from oscillations in vascular smooth muscle cell CFTR expression.

To our knowledge, we are the first to (1) assess myogenic reactivity with the necessary time resolution to conduct a cycle analysis and (2) demonstrate that cerebrovascular myogenic tone oscillates with a circadian rhythm. There is evidence that circadian rhythms in myogenic reactivity may vary across vascular beds, although the available data are admittedly sparse. For example, total peripheral resistance displays a circadian rhythm,[21] but this rhythm is antiphase to the cerebrovascular
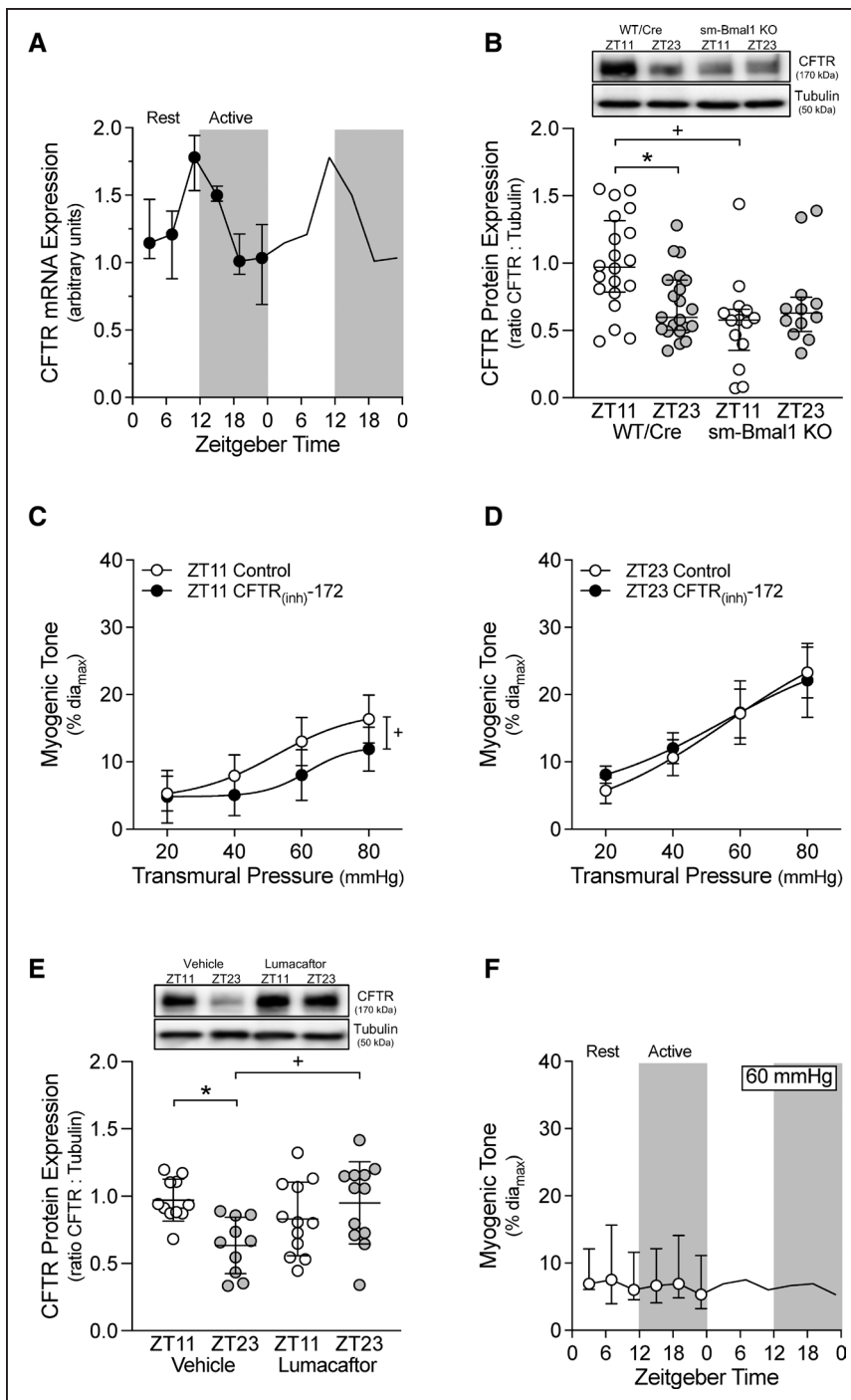
Figure 5. Oscillations in CFTR (cystic fibrosis transmembrane conductance regulator) expression associate with cerebral artery myogenic tone.
A, Olfactory cerebral artery CFTR mRNA expression is plotted over Zeitgeber time (ZT; n=4 at each ZT point). CFTR mRNA expression exhibits a statistically significant circadian rhythm (JTK_CYCLE $P<0.05$). **B**, In olfactory arteries isolated from tamoxifen-treated, Cre-expressing control mice (Cre-expressing wild-type control [tamoxifen treated; WT/Cre]; n=20–21), CFTR protein expression is higher at ZT11 than at ZT23. This differential expression does not occur in arteries isolated from smooth muscle cell–specific Bmal1 (brain and muscle aryl hydrocarbon receptor nuclear translocator-like protein 1) knockout mice (sm-Bmal1 KO; n=12–14). In sm-Bmal1 KO arteries, CFTR expression at ZT11 is reduced to the ZT23 level. Inhibiting CFTR channel activity (100 nmol/L CFTR$_{(inh)}$-172 for 30 min in vitro) attenuates myogenic tone at **(C)** ZT11 (n=5; paired comparison), but not (**D**) ZT23 (n=5; paired comparison). **D**, Lumacaftor treatment in vivo (3 mg/[kg·day] IP for 2 d) eliminates the difference in CFTR protein expression at ZT11/ZT23 (n=10–12); in lumacaftor-treated mice, CFTR expression at ZT23 is elevated to the ZT11 level. **E**, Myogenic tone at 60 mm Hg in arteries isolated from lumacaftor-treated mice is plotted over Zeitgeber time (n=5–6 at each Zeitgeber time point). Myogenic tone does not exhibit a circadian rhythm (JTK_CYCLE P=not significant). In **A** and **F**, data are presented as medians±interquartile range and are double-plotted for visualization purposes; white shading indicates lights on and dark shading indicates lights off. Western blot data in **B** are presented as medians±interquartile range and analyzed with a Kruskal-Wallis test with Dunn post-test. $^{*}P<0.05$ for ZT11 vs ZT23 and $+P<0.05$ for control vs manipulation at either ZT11 or ZT23.

rhythm we report here. Mesenteric artery myogenic tone is higher at ZT7 compared with ZT19,[22] again a pattern that clearly differs from the cerebrovascular rhythm we report. The molecular signaling mechanisms underlying myogenic reactivity can differ substantively across vascular beds[23]: the molecular clock, therefore, could drive distinct rhythms by capitalizing on this heterogeneity and intersecting with the distinct molecular mediators within each vascular bed. By extension, understanding how the molecular clock modulates myogenic reactivity in a given vascular bed would potentially open novel opportunities

to therapeutically target myogenic reactivity in a vascular bed–specific manner.

Mechanistically, our data suggest that rhythmic CFTR expression drives the oscillations in myogenic reactivity in the wild-type setting: in this regard, our previous observation that skeletal muscle resistance artery myogenic tone is not sensitive to CFTR manipulation[7] is consistent with the postulate that circadian regulators of myogenic reactivity vary across vascular beds. Few studies have explored whether CFTR expression is rhythmic in other tissues and the currently available data
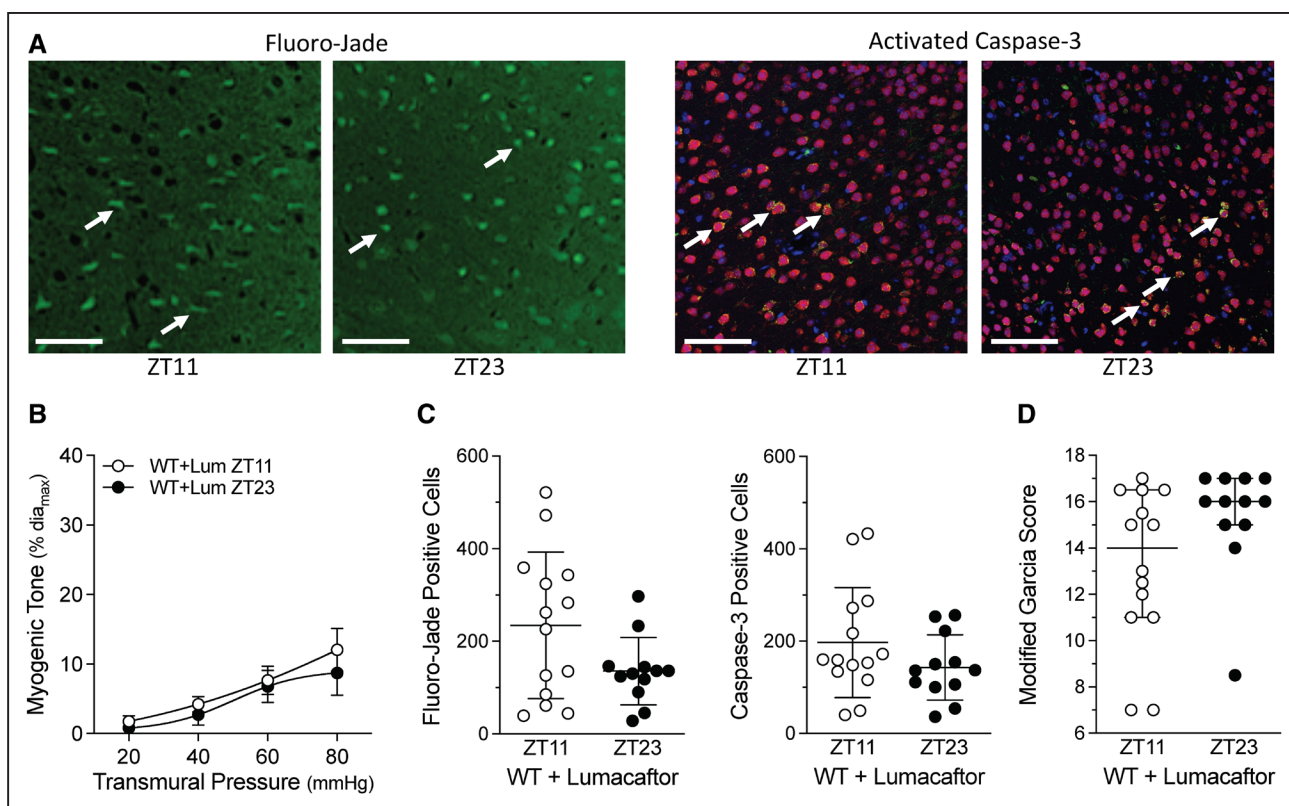
Figure 6. Subarachnoid hemorrhage (SAH)–induced injury in mice pretreated with lumacaftor.
Mice were pretreated with lumacaftor (3 mg/[kg·d] IP; Lum) for 2 d; following pretreatment, SAH was induced at Zeitgeber Time 11 (ZT11) or Zeitgeber time 23 (ZT23). Behavioral assessments and tissue collection were conducted 48 h afterwards. **A**, Shows representative images of cortical cells stained with Fluoro-Jade (**left**) and for activated caspase-3 expression (**right**); arrows point to positively stained cells (Bar=60 μm). **B**–**D**, Show the association between myogenic tone at the time of SAH and the resulting injury that ensues. **B**, Before the SAH surgery, olfactory cerebral artery myogenic tone is similar at ZT11 and ZT23 (n=5). **C**, Positive cell counts for Fluoro-Jade staining and activated caspase-3 are similar in lumacaftor pretreated mice when SAH is induced at ZT1 vs ZT23 (n=12–14). **D**, Modified Garcia scores in lumacaftor pretreated mice are similar when SAH is induced at ZT11 vs ZT23 (n=12–14). Modified Garcia scores in **D** are presented as medians±interquartile range and compared with a Mann-Whitney test. WT indicates wild-type.

are contradictory.[24,25] To our knowledge, no studies have identified specific interactions between molecular clock transcription factors (eg, Bmal1) and the CFTR gene.

Our study independently confirms the existence of time-of-day differences in SAH-induced neuronal injury and microglial cell activation, with higher levels occurring near the night-to-day transition (ie, ZT2 in Schallner et al[2] and ZT23 here). We extended these observations, with the use of alternate markers of neuronal injury, the addition of neurological assessments, and in vitro vascular reactivity studies. Furthermore, we separated our time points by 12 hours, since circadian rhythms oscillate with a 24-hour period, and thus, the peak and trough should be 12 hours apart.

Higher cerebral artery myogenic tone should reduce brain perfusion: thus, if a vascular mechanism influences SAH-induced injury, the injury level should be higher at ZT23, compared to ZT11. Indeed, higher levels of neuronal injury and lower neurological scores are observed when SAH is induced at ZT23 versus ZT11. Smooth muscle cell clock disruption (sm-Bmal1 KO) eliminates the circadian rhythm in myogenic reactivity,

indicating that this rhythm emanates from the smooth muscle cell molecular clock. Interestingly, the sm-Bmal1 KO myogenic reactivity profile displays an isolated peak at ZT11 that flips the ZT11/ZT23 myogenic tone relationship in sm-Bmal1 KO cerebral arteries, relative to wild-type arteries: remarkably, neuronal injury and neurological scores similarly invert, thereby strengthening the observed relationship between cerebrovascular myogenic tone and SAH-induced injury. CFTR expression in sm-Bmal1 KO cerebral arteries is similar at ZT11 and ZT23, indicating that a CFTR-independent mechanism underlies the higher myogenic tone at ZT11. Although the molecular mechanism remains unknown, it is likely due to the actions of an external, non-smooth muscle–derived stimulus that is normally overridden in the wild-type setting.

Schallner et al[2] proposed that microglial cell activation could potentially mediate the time-of-day differences in SAH-induced injury. However, the sm-Bmal1 KO model does not alter the cortical microglial cell activation pattern, although it does alter neuronal injury. This indicates that microglial activation is (1) not the primary

determinant of time-of-day differences in SAH-induced injury and (2) not coupled to the reduced perfusion that presumably results from the ZT11/ZT23 difference in vascular reactivity. These data add yet another layer of evidence that the time-dependent difference in SAH-induced neuronal injury is vascular in origin. Furthermore, because we did not observe a time-of-day difference in large artery vasoconstriction, our data localize this vascular effect to the cerebral microcirculation. Given that the cerebral microcirculation is the largest contributor to cerebrovascular resistance,[8] variations in microvascular myogenic reactivity are undoubtedly capable of modulating cerebral perfusion and SAH-induced ischemic injury.

The primary implication of this circadian study is that microvascular constriction within the initial hours following SAH plays a crucial role in the injury level. This extends the therapeutic window for microvascular interventions to a much earlier time point than the emergence of delayed cerebral ischemia (the latter is the current microvascular research focus for SAH[1]). A second implication is that it is important to assess whether microvascular interventions are efficacious at all times of the day or predominantly at the end of the active phase, when cerebrovascular constriction is normally highest. Indeed, several neuroprotective interventions have failed to deliver clinical benefit, in part because the circadian rhythms of the nocturnal animal models do not properly align with those of the target patient population.[26] Thus, it is crucial to incorporate the circadian dimension into stroke research and therapy design.[4,26,27]

Although beyond the scope of the present study, it is worth noting that SAH disrupts circadian rhythms within the brain as a component of the pathology.[2] This aspect has not been comprehensively studied and consequently, it is not clear to what extent circadian rhythm disruption per se contributes to the SAH pathology. As a future direction, it would be intriguing to examine whether SAH disrupts the microvascular rhythm in myogenic reactivity and whether therapeutically targeting this disruption would provide benefit. In this regard, several interventions, including glucagon-like peptide-1 receptor agonism[28] and retinoic acid receptor-related orphan receptor alpha agonism (a nuclear receptor for melatonin)[29] are proposed to modulate/restore disrupted rhythms in neuropathological settings.

In summary, multiple factors contribute to pathological injury after SAH; however, there is little doubt that microvascular constriction and ischemia are significant contributors. This study identifies circadian rhythmicity in cerebral artery myogenic reactivity as a key factor influencing SAH-induced injury. By identifying rhythmic CFTR expression as the mechanism underpinning the cerebrovascular myogenic reactivity rhythm, it becomes feasible to therapeutically manipulate both the microvascular rhythm and the time-of-day differential in SAH injury. Our investigation incorporates important circadian mechanisms into the pathological concept of SAH-induced neurological injury.

REFERENCES

1. Solenski NJ, Haley EC Jr, Kassell NF, Kongable G, Germanson T, Truskowski L, Torner JC. Medical complications of aneurysmal subarachnoid hemorrhage: a report of the multicenter, cooperative aneurysm study. Participants of the Multicenter Cooperative Aneurysm Study. *Crit Care Med.* 1995;23:1007–1017. doi: 10.1097/00003246-199506000-00004

2. Schallner N, Lieberum JL, Gallo D, LeBlanc RH 3rd, Fuller PM, Hanafy KA, Otterbein LE. Carbon monoxide preserves circadian rhythm to reduce the severity of subarachnoid hemorrhage in mice. *Stroke.* 2017;48:2565–2573. doi: 10.1161/STROKEAHA.116.016165

3. Zhang R, Lahens NF, Ballance HI, Hughes ME, Hogenesch JB. A circadian gene expression atlas in mammals: implications for biology and medicine. *Proc Natl Acad Sci USA.* 2014;111:16219–16224. doi: 10.1073/pnas.1408886111

4. Lo EH, Albers GW, Dichgans M, Donnan G, Esposito E, Foster R, Howells DW, Huang YG, Ji X, Klerman EB, et al. Circadian biology and stroke. *Stroke.* 2021;52:2180–2190. doi: 10.1161/STROKEAHA.120.031742

5. Li D, Ma S, Guo D, Cheng T, Li H, Tian Y, Li J, Guan F, Yang B, Wang J. Environmental circadian disruption worsens neurologic impairment and inhibits hippocampal neurogenesis in adult rats after traumatic brain injury. *Cell Mol Neurobiol.* 2016;36:1045–1055. doi: 10.1007/s10571-015-0295-2. Published Erratum: *Cell Mol Neurobiol.* 2021;41:615-616. doi: 10.1007/s10571-020-00913-3

6. Yagi K, Lidington D, Wan H, Fares JC, Meissner A, Sumiyoshi M, Ai J, Foltz WD, Nedospasov SA, Offermanns S, et al. Therapeutically targeting tumor necrosis factor-α/sphingosine-1-phosphate signaling corrects myogenic reactivity in subarachnoid hemorrhage. *Stroke.* 2015;46:2260–2270. doi: 10.1161/STROKEAHA.114.006365

7. Lidington D, Fares JC, Uhl FE, Dinh DD, Kroetsch JT, Sauvé M, Malik FA, Matthes F, Vanherle L, Adel A, et al. CFTR therapeutics normalize cerebral perfusion deficits in mouse models of heart failure and subarachnoid hemorrhage. *JACC Basic Transl Sci.* 2019;4:940–958. doi: 10.1016/j.jacbts.2019.07.004

8. Mulvany MJ, Aalkjaer C. Structure and function of small arteries. *Physiol Rev.* 1990;70:921–961. doi: 10.1152/physrev.1990.70.4.921

9. Gerashchenko D, Matsumura H. Continuous recordings of brain regional circulation during sleep/wake state transitions in rats. *Am J Physiol.* 1996;270(4 pt 2):R855–R863. doi: 10.1152/ajpregu.1996.270.4.R855

10. Wauschkuhn CA, Witte K, Gorbey S, Lemmer B, Schilling L. Circadian periodicity of cerebral blood flow revealed by laser-Doppler flowmetry in awake rats: relation to blood pressure and activity. *Am J Physiol Heart Circ Physiol.* 2005;289:H1662–H1668. doi: 10.1152/ajpheart.01242.2004

11. Madsen PL, Schmidt JF, Wildschiødtz G, Friberg L, Holm S, Vorstrup S, Lassen NA. Cerebral O2 metabolism and cerebral blood flow in humans during deep and rapid-eye-movement sleep. *J Appl Physiol (1985).* 1991;70:2597–2601. doi: 10.1152/jappl.1991.70.6.2597

12. Manfredini R, Boari B, Smolensky MH, Salmi R, la Cecilia O, Maria Malagoni A, Haus E, Manfredini F. Circadian variation in stroke onset: identical temporal pattern in ischemic and hemorrhagic events. *Chronobiol Int.* 2005;22:417–453. doi: 10.1081/CBI-200062927

13. Storch KF, Paz C, Signorovitch J, Raviola E, Pawlyk B, Li T, Weitz CJ. Intrinsic circadian clock of the mammalian retina: importance for retinal processing of visual information. *Cell.* 2007;130:730–741. doi: 10.1016/j.cell.2007.06.045

14. Wirth A, Benyó Z, Lukasova M, Leutgeb B, Wettschureck N, Gorbey S, Orsy P, Horváth B, Maser-Gluth C, Greiner E, et al. G12-G13-LARG-mediated signaling in vascular smooth muscle is required for salt-induced hypertension. *Nat Med.* 2008;14:64–68. doi: 10.1038/nm1666

15. Wan H, Wang Y, Ai J, Brathwaite S, Ni H, Macdonald RL, Hol EM, Meijers JCM, Vergouwen MDI. Role of von Willebrand factor and ADAMTS-13 in early brain injury after experimental subarachnoid hemorrhage. *J Thromb Haemost.* 2018;16:1413–1422. doi: 10.1111/jth.14136

16. Davis BM, Salinas-Navarro M, Cordeiro MF, Moons L, De Groef L. Characterizing microglia activation: a spatial statistics approach to maximize information extraction. *Sci Rep.* 2017;7:1576. doi: 10.1038/s41598-017-01747-8

17. Hughes ME, Hogenesch JB, Kornacker K. JTK_CYCLE: an efficient nonparametric algorithm for detecting rhythmic components in genome-scale data sets. *J Biol Rhythms.* 2010;25:372–380. doi: 10.1177/0748730410379711

18. Rudic RD, McNamara P, Reilly D, Grosser T, Curtis AM, Price TS, Panda S, Hogenesch JB, FitzGerald GA. Bioinformatic analysis of circadian gene oscillation in mouse aorta. *Circulation.* 2005;112:2716–2724. doi: 10.1161/CIRCULATIONAHA.105.568626

19. Meissner A, Yang J, Kroetsch JT, Sauvé M, Dax H, Momen A, Noyan-Ashraf MH, Heximer S, Husain M, Lidington D, et al. Tumor necrosis factor-α-mediated downregulation of the cystic fibrosis transmembrane conductance regulator drives pathological sphingosine-1-phosphate signaling in a mouse model of heart failure. *Circulation.* 2012;125:2739–2750. doi: 10.1161/CIRCULATIONAHA.111.047316

20. Nelson MT, Conway MA, Knot HJ, Brayden JE. Chloride channel blockers inhibit myogenic tone in rat cerebral arteries. *J Physiol.* 1997;502 (pt 2):259–264. doi: 10.1111/j.1469-7793.1997.259bk.x

21. Smith TL, Coleman TG, Stanek KA, Murphy WR. Hemodynamic monitoring for 24 h in unanesthetized rats. *Am J Physiol.* 1987;253(6 pt 2):H1335–H1341. doi: 10.1152/ajpheart.1987.253.6.H1335

22. Xie Z, Su W, Liu S, Zhao G, Esser K, Schroder EA, Lefta M, Stauss HM, Guo Z, Gong MC. Smooth-muscle BMAL1 participates in blood pressure circadian rhythm regulation. *J Clin Invest.* 2015;125:324–336. doi: 10.1172/JCI76881

23. Lidington D, Schubert R, Bolz SS. Capitalizing on diversity: an integrative approach towards the multiplicity of cellular mechanisms underlying myogenic responsiveness. *Cardiovasc Res.* 2013;97:404–412. doi: 10.1093/cvr/cvs345

24. Hoogerwerf WA, Sinha M, Conesa A, Luxon BA, Shahinian VB, Cornélissen G, Halberg F, Bostwick J, Timm J, Cassone VM. Transcriptional profiling of mRNA expression in the mouse distal colon. *Gastroenterology.* 2008;135:2019–2029. doi: 10.1053/j.gastro.2008.08.048

25. Soták M, Polidarová L, Musílková J, Hock M, Sumová A, Pácha J. Circadian regulation of electrolyte absorption in the rat colon. *Am J Physiol Gastrointest Liver Physiol.* 2011;301:G1066–G1074. doi: 10.1152/ajpgi.00256.2011

26. Esposito E, Li W, Mandeville ET, Park JH, Şencan I, Guo S, Shi J, Lan J, Lee J, Hayakawa K, Sakadžić S, Ji X, Lo EH. Potential circadian effects on translational failure for neuroprotection. *Nature.* 2020;582:395–398. doi: 10.1038/s41586-020-2348-z

27. Boltze J, Didwischus N, Merrow M, Dallmann R, Plesnila N. Circadian effects on stroke outcome - Did we not wake up in time for neuroprotection? *J Cereb Blood Flow Metab.* 2021;41:684–686. doi: 10.1177/0271678X20978711

28. Wang L, Zhao J, Wang CT, Hou XH, Ning N, Sun C, Guo S, Yuan Y, Li L, Hölscher C, Wang XH. D-Ser2-oxyntomodulin ameliorated Aβ31-35-induced circadian rhythm disorder in mice. *CNS Neurosci Ther.* 2020;26:343–354. doi: 10.1111/cns.13211

29. Farahani S, Solgi L, Bayat S, Abedin Do A, Zare-Karizi S, Safarpour Lima B, Mirfakhraie R. RAR-related orphan receptor A: one gene with multiple functions related to migraine. *CNS Neurosci Ther.* 2020;26:1315–1321. doi: 10.1111/cns.13453